

Journal Pre-proof

A new approach to analytical modelling of groyne fields

Antonios Valsamidis, Dominic E. Reeve



PII: S0278-4343(20)30243-0

DOI: <https://doi.org/10.1016/j.csr.2020.104288>

Reference: CSR 104288

To appear in: *Continental Shelf Research*

Received Date: 23 October 2019

Revised Date: 26 June 2020

Accepted Date: 25 October 2020

Please cite this article as: Valsamidis, A., Reeve, D.E., A new approach to analytical modelling of groyne fields, *Continental Shelf Research* (2020), doi: <https://doi.org/10.1016/j.csr.2020.104288>.

This is a PDF file of an article that has undergone enhancements after acceptance, such as the addition of a cover page and metadata, and formatting for readability, but it is not yet the definitive version of record. This version will undergo additional copyediting, typesetting and review before it is published in its final form, but we are providing this version to give early visibility of the article. Please note that, during the production process, errors may be discovered which could affect the content, and all legal disclaimers that apply to the journal pertain.

© 2020 Published by Elsevier Ltd.

1

2

A new approach to analytical modelling of groyne fields

3

4

Antonios Valsamidis, Dominic E. Reeve*

5

*Zienkiewicz Centre for Computational Engineering, College of Engineering,
Swansea University, Fabian Way, Swansea, SA1 8EN, UK

6

7

8 **Abstract**

9 Analytical and computational techniques for finding solutions to the equations
10 describing shoreline evolution are widely known and the advantages and
11 disadvantages of both are well documented. Initial analytical solutions to the 1-line
12 models were restricted to constant wave conditions and simple beach/structure
13 configurations. Recent developments in analytical treatments have allowed solutions
14 to be found for an arbitrary sequence of wave conditions, but again for simple
15 configurations. Here, we propose a method of linking several analytical solutions
16 together in order to describe the unsteady evolution of a beach within a groyne field,
17 allowing for both permeability of the groynes and by-passing. The method relies on
18 specifying boundary conditions in each groyne cell that mimic the transmission and
19 by-passing of sediment. The conditions are generalisations of boundary conditions
20 that are well-known. Solutions for groyne fields on straight and convex shorelines are
21 presented to illustrate the method for constant and time varying wave conditions.

22 **Keywords:** groyne, groyne-field, shoreline evolution, erosion, coastal defence
23 scheme

24 **1. Introduction**

25 **1.1. Background**

26 Groynes are elongated coastal structures placed normal to the shore. They are
27 usually made of timber, concrete or rock and their purpose is to interrupt the wave-
28 driven longshore transport of sand along the beach in order to mitigate erosion.
29 However, given a predominant longshore drift, accretion is expected on the updrift
30 side of the groyne and erosion on the downdrift side, due to the blockage of longshore
31 sediment transport by the groyne. Thus the application of groynes as a means of

32 coastal protection is only partly effective as every area of accretion is balanced by a
33 corresponding area of erosion. Extremes of accretion and erosion can be avoided by
34 placing a sequence of groynes along a stretch of beach between two control points
35 such as headlands which place a natural limit on the movement of sand. Alternatively,
36 on a long open stretch of beach groyne fields might be constructed to taper the
37 amount of sediment retained by the groynes near the edge of the groyne field. In this
38 case, reducing the length of the groyne promotes bypassing of sand around the
39 seaward tip, reducing the height allows sediment in suspension to overtop the groyne
40 and increasing the permeability allows the transmission of sediment through the trunk
41 of the groyne, as illustrated in Fig. 1.

42 Figure 1

43 It is, as a result, not uncommon to see series of groynes along a beach. Such an
44 arrangement is called a groyne field; and example is shown in Fig. 2.

45 Figure 2

46 A groyne field must be carefully designed to maintain the sediment material in
47 the beach fronting the area being protected. Specifically, if the groyne length is too
48 short sediment bypassing at the tips of the groynes may occur to an excessive degree
49 resulting in poor sediment retention, (Coghlan et al., 2013). If the groynes are too long
50 or too high or impermeable (e.g. mass concrete), an inadequate amount of sediment
51 flow may pass to their downdrift side, and consequently, the sediment material which
52 has already been lost in this area will not be replaced causing erosion downdrift of the
53 groynes, (Hanson et al., 2008).

54 Terminal groyne syndrome refers to the erosion which is expected to occur
55 downdrift of the terminal groyne in a groyne field. Examples of extreme negative
56 impacts of this phenomenon include Southwick beach in West Sussex, UK, as shown
57 in Fig3a, (Clarke et al., 2017), as well as Westhampton beach in New York, shown in
58 Fig3b, (Dean and Dalrymple, 2002).

59 Figure 3

60 Further details of principles governing groyne design may be found in Fleming
61 (1990), Kraus et al. (1994), Basco and Pope (2004). Here, our focus is on techniques
62 to assist in predicting how a beach will respond to the construction of a groyne field.

63 1.2 Beach Model Background

64 The One-Line model, a simplified physics-based model, is generally used for
65 simulating medium to long-term shoreline morphodynamic evolution, on shorefronts
66 extending up to approximately *30 km*, (Gravens et al., 1991). The One-Line model has
67 successfully served over time as a robust and reliable tool for assessing beach
68 morphodynamic evolution, (e.g. US Army Corps, 2002), and is considered a suitable
69 tool for testing the performance of groyne-fields for certain wave and hydrodynamic
70 conditions with respect to specific beaches, and for a variety of different geometric
71 parameters as far as the groyne length, groyne permeability and groyne spacing is
72 concerned.

73 The One-Line model is based on a combination of the continuity of mass
74 equation and a longshore sediment transport equation (e.g. Larson et al., 1987). The
75 primary assumptions are: (a) the beach profile is in equilibrium and is unchanging in
76 time, (this implies the bathymetric contours are parallel to each other so that one
77 contour is sufficient to predict the entire beach movement; (b) The longshore
78 sediment transport takes place up to a specific depth, the depth of closure D_c . No
79 longshore sediment transport is considered to occur seaward of this.

80 Early analytical solutions to the One-Line Model were based on the
81 assumption of constant wave forcing, mild shoreline gradient and small wave angle
82 with respect to the shoreline orientation. With these restrictions the equations may be
83 condensed into a single diffusion-type equation (Eq. (1)), (Pelnard-Considère ,1956):

$$84 \frac{\partial y}{\partial t} = \varepsilon \frac{\partial^2 y}{\partial x^2} \quad (1)$$

85 where x is the longshore distance on an axis X parallel to the shoreline trend, y is the
86 shoreline position on a Y axis vertical to X , ε is the diffusion coefficient, and t is time.

87 Computational integration of the one-line model is based on the simultaneous
88 solution of three equations: continuity; longshore transport; and a geometrical
89 expression relating the wave and beach angles. Time varying wave conditions, larger
90 wave angles and nearshore wave transformation such as diffraction can be
91 incorporated into computational schemes to enhance their general applicability, (see
92 e.g. Gravens et al., 1991). They have been used to investigate the evolution of more
93 complex situations such as groyne fields, and for design purposes.

94 The one-line framework can also be extended to include one or more
95 additional contours in order to provide a better description of the cross-shore variation
96 in the dynamics. Nevertheless, the cross-shore exchange of sediment between the
97 contours is usually parameterised in the form of a relaxation towards an equilibrium
98 shape. Two-line models, in the form of the analytical approach of Bakker (1969) and
99 the computational solution of Horikawa et al (1979) provided the simplest description
100 of changes in beach slope, while the multi-line, (or N-line), models proposed by
101 Perlin & Dean (1979, 1983) and Steetzel et al. (1988) provided additional fidelity to
102 the description of cross-shore transport dynamics. However, N-line models have yet
103 to find wide acceptance and usage in practice. This has been attributed to the greater
104 data demands they make and, to a lesser extent, the longer computing time they
105 require. Another reason may be their susceptibility to numerical instability noted by
106 Perlin & Dean (1983) and Shibutani et al (2009). Their inherent instability under
107 certain conditions was subsequently established by Reeve & Valsamidis (2014) for
108 small wave and shoreline angles.

109 On the other hand, analytical solutions to the One-Line model can be utilized
110 for isolating and remotely studying specific coastal phenomena, and consequently
111 validating testing computational models, (Hanson, 1987). Further, analytical solutions
112 can be evaluated immediately for any chosen time, rather than timestepping over
113 many small intervals as in computational approaches. With additional efforts,
114 researchers have loosened some of the fundamental restrictions of analytical
115 solutions. For instance, Larson et al. (1997) produced an analytical solution to the
116 One-Line Model, via Laplace transform techniques, for a single groyne and a groyne-
117 compartment, assuming sinusoidally time-varying wave angle. An approximate
118 method for allowing arbitrary time varying conditions was proposed by Walton and
119 Dean (2011) and Valsamidis et al. (2013). This combined previous analytical
120 solutions for constant wave conditions with a Heaviside scheme to allow a solution
121 for arbitrarily varying wave time-series to be constructed. The same approach was
122 adopted by Valsamidis and Reeve (2017) to develop solutions for the case of a beach
123 with a groyne and a river-mouth, with the latter acting as a source or sink of sediment
124 discharge influencing the shoreline evolution near the groyne.

125 Analytical solutions to Eq. (1) produced via Fourier transform techniques can
126 include time-varying wave conditions without needing modifications such as the

127 application of a Heaviside scheme to do so. Reeve (2006) presented an analytical
 128 solution, based on Fourier transform techniques, for the case of an impermeable
 129 groyne on an arbitrary initial shoreline shape subject to arbitrarily varying wave
 130 conditions. The solution was presented in the form of integrals that required
 131 numerical evaluation to capture the effect of arbitrary wave conditions. Such kinds of
 132 solutions have been termed ‘semi-analytical’ because although they are derived
 133 analytically, they require numerical integration for their evaluation. In this paper we
 134 extend the range of applicability of semi-analytical solutions by proposing new
 135 boundary conditions that mimic by-passing around the groyne tip and groyne
 136 permeability, as well as extending solutions to describe a groyne field.

137

138 2. Methodology

139 The strategy is to combine semi-analytical solutions for a single groyne and a
 140 groyne compartment to form a model suitable for describing an extended groyne field.
 141 Specifically, the semi-analytical solution regarding shoreline evolution near a groyne
 142 (Reeve, 2006) was coupled with the one derived by Zacharioudaki and Reeve (2008)
 143 for a groyne compartment, with an appropriate internal boundary condition.

144 2.1 The semi-analytical solution for shoreline evolution near a groyne

145 Reeve (2006) used a Fourier cosine transform to develop a solution to Eq. (1)
 146 for arbitrary initial beach shape and wave conditions for shoreline evolution near a
 147 groyne.

148 Figure 4

149 This solution consists of the sum of the following 3 terms:

$$150 \quad y_1^G = \frac{1}{\pi} (\pi \int_0^t \varepsilon(u) du)^{-1/2} \int_0^{+\infty} g(\xi) \left[\exp\left(-\frac{(x-\xi)^2}{4 \int_0^t \varepsilon(u) du}\right) + \exp\left(-\frac{(x+\xi)^2}{4 \int_0^t \varepsilon(u) du}\right) \right] d\xi \quad (2)$$

151 where $g(x)$ is the initial shoreline position, and ξ is a dummy variable used in the
 152 integration process. In many cases the initial beach is taken as a straight line with
 153 $g(x)=0$ in which case this term is identically zero. y_1^G describes the contribution of the
 154 initial shoreline shape to the consequent evolution;

$$155 \quad y_2^G = \frac{2}{\pi} \int_0^{+\infty} \left(\int_0^t \exp(-\int_w^t [\omega^2 \varepsilon(u)] du) \tilde{q}(\omega, w) dw \right) \cos(\omega x) d\omega \quad (3)$$

156 where ω is the transform variable used in the Fourier cosine transform operation, \tilde{q} is
 157 the Fourier cosine transformed variable of q ; the latter parameter describes the
 158 sediment flow from a source or sink of sediment discharge, and w is a variable related
 159 to time. Again, in case that there are no sources or sinks $q(t)$ may be considered equal
 160 to zero, and the second term is zero as well. This term corresponds to the impact of a
 161 source or sink of sediment discharge on shoreline evolution;

$$162 \quad y_3^G = \frac{1}{\sqrt{\pi}} \int_0^t \varepsilon(w) j(w) \left(\frac{1}{\sqrt{\pi \int_w^t \varepsilon(u) du}} \exp\left(-\frac{x^2}{4 \int_w^t \varepsilon(u) du}\right) \right) dw \quad (4)$$

163 where $j(w)$ is the boundary condition at the groyne. The third term y_3^G corresponds to
 164 the impact of the combination of wave action and the boundary condition at the
 165 groyne on the shoreline evolution. If the time variation of $\varepsilon(t)$ has a specified
 166 functional form, the integration of Eq. (4) may be performed analytically.
 167 Alternatively, if $\varepsilon(t)$ is specified by an arbitrary time-series then the integrals must be
 168 evaluated numerically.

169 Finally, the shoreline position is given as the summation of Eqs. (2), (3) and
 170 (4):

$$171 \quad y^G = y_1^G + y_2^G + y_3^G \quad (5)$$

172 The semi-analytical solution has been tested, for a range of simple conditions, against
 173 analytical solutions by Valsamidis (2016) and Valsamidis and Reeve (2017).

174

175 2.2 The semi-analytical solution for a groyne compartment

176 Zacharioudaki and Reeve (2008) provided a semi-analytical solution to the
 177 One-Line model for the case of shoreline evolution in a groyne compartment (Fig. 5):

178 Figure 5

179 The shoreline evolution in a groyne compartment is described by a solution to
 180 Eq. 1, which is derived via finite Fourier cosine transforms. This solution comprises
 181 of the following 4 terms:

$$182 \quad y_1^{GC} = \frac{1}{a} \bar{g}(0) + \frac{1}{a} \int_0^t \varepsilon(w) (j(w) - k(w) + \hat{s}(0, w)) dw \quad (6)$$

$$183 \quad y_2^{GC} = \frac{2}{a} \sum_{\psi=1}^{+\infty} \cos\left(\frac{\psi\pi x}{a}\right) \hat{g}(\psi) \exp\left(-\int_0^t \frac{\pi^2 \psi^2}{a^2} \varepsilon(u) du\right) \quad (7)$$

$$y_3^{GC} = \frac{2}{a} \sum_{\psi=1}^{+\infty} \cos\left(\frac{\psi\pi x}{a}\right) \int_0^t \exp\left(-\int_w^t \varepsilon(u) \left(\frac{\psi\pi}{a}\right)^2 du\right) (\varepsilon(u) \left((-1)^\psi j(w) - k(w)\right)) dw$$
(8)

$$y_4^{GC} = \frac{2}{a} \sum_{\psi=1}^{+\infty} \cos\left(\frac{\psi\pi x}{a}\right) \int_0^t \exp\left(-\int_w^t \varepsilon(u) \left(\frac{\psi\pi}{a}\right)^2 du\right) \hat{s}(\psi, w) dw$$
(9)

In the above equations $g(x)$ corresponds to the initial shoreline position, $\hat{g}(\psi) = \int_0^a g(x) \cos\left(\frac{\psi\pi x}{a}\right) dx$ thus, $\hat{g}(0) = \int_0^a g(x) dx$; 'a' refers to the groyne compartment's length; $\hat{g}(\psi)$ is the finite-Fourier cosine transform of $g(x)$; ψ is an integer transform variable; $j(w)$ is the time-varying boundary condition on the left side of the groyne compartment; $k(w)$ is the corresponding boundary condition on the right side of the groyne compartment; w is a dummy variable of integration running from time 0 to arbitrary time t . The integrals with respect to u yield a number for a given value of t while those with respect to w require numerical evaluation. Finally, the source term appearing in Eq. 6 is given by: $\hat{s}(0, w) = \int_0^a s(x, w) dx$

The term y_2^{GC} incorporates the initial shoreline shape while y_3^{GC} the boundary conditions at the groynes. The source term is described by the fourth term y_4^{GC} . However, the term y_1^{GC} involves the initial shoreline position, the source term and the boundary conditions. Finally, the shoreline evolution in a groyne compartment is given by the summation of Eqs. (6)-(9):

$$y^{GC} = y_1^{GC} + y_2^{GC} + y_3^{GC} + y_4^{GC}$$
(10)

where $j(w)$ and $k(w)$ are the boundary conditions on the left-hand side and right-hand side groynes of the groyne compartment, respectively.

2.3 A new internal boundary condition for combining different solutions

A groyne field can be considered as the concatenation of single groynes and groyne compartments. The solutions for these cases may be combined to give a solution for a groyne field as shown in (Fig. 6):

Figure 6

Thus, a groyne field might be modelled for a chosen number of groynes, with the option to consider open external boundaries, and as initial condition, an arbitrary shoreline shape (Fig. 7):

212 Figure 7

213 Early analytical solutions treated the case of impermeable groynes of infinite
 214 length. Here we seek an internal boundary condition that reflects real life more
 215 closely. That is, a condition that allows sediment transport to take place through and
 216 around groynes. In other words, a condition that mimics groynes of finite length that
 217 are permeable with the potential of sediment bypassing around their seaward tip.
 218 Hanson (1989) proposed the following formula for describing the portion of
 219 longshore sediment flux ra that bypasses a groyne (Eq. (10)):

$$220 \quad ra = 1 - \frac{D_G}{D_{LT}} \quad \text{considering } D_{LT} > D_G \quad (11)$$

221 However, if $D_{LT} \leq D_G$, then $ra=0$,

222 where D_G is the depth at the groyne's tip and D_{LT} is the depth of active longshore
 223 transport. The latter is given by the formula (Hanson, 1989):

$$224 \quad D_{LT} = \frac{1.27}{\gamma} (H_{s,b}) \quad (12)$$

225 where γ is the breaking wave index and here was taken equal to 0.78, while $H_{s,b}$ is the
 226 significant wave height at breaking position. Eq. (11) is postulated on the assumption
 227 that the longshore transport is distributed uniformly across the active profile. As
 228 Hanson (1989) noted, a thorough analysis of sand transport around groynes would
 229 require the cross-shore distribution of the longshore sand transport rate, as well as the
 230 2-d horizontal pattern of sand transport. In the absence of a reliable predictive
 231 expression to account for this Eq. (11) is the simplest assumption giving reasonable
 232 results. There remains a lack of reliable predictive expressions, verified under
 233 prototype conditions, so we have adopted this pragmatic approach here. As is clear
 234 from Eq. (12), D_{LT} , the offshore-ward limit of longshore sediment movement, varies
 235 in time according to the corresponding significant wave height value in a sequence of
 236 wave events. The relationship between D_c and D_{LT} is best considered in terms of time
 237 scale. D_c is usually defined in terms of an extreme wave height, corresponding to
 238 storm conditions experienced once every few years. D_{LT} defines the instantaneous
 239 value of the seaward extent of the active profile. Under extreme conditions it will
 240 equal D_c , but under calmer ones it will be smaller than D_c . The concept of D_c is
 241 inextricably linked to wave height, and thus the period over which wave heights are
 242 measured to determine their maximum value. A longer period of observation is more

243 likely to include a major storm event in which the cross-shore profile is altered, thus
 244 leading to a greater value of D_c . In practice there is a finite limit to the length of
 245 records and a pragmatic choice for D_c has to be made. Various authors have suggested
 246 formulae, (e.g. Birkemeier 1985), but all are quite close to the formulation of
 247 Hallermeier (1983) that gives the annual depth of closure as being approximately
 248 twice the annual maximum wave height.

249 However, as the depth at the groyne tip, D_G , may change in time due to the
 250 shoreline movement, and in addition, D_G may be different on the updrift and
 251 downdrift side off the groyne, Eq. (11) cannot be applied without taking into
 252 consideration a time-varying D_G (Fig. 8):

253 Figure 8

254 Consequently, a time-varying water depth $D_G(t)$ is introduced in this study, assuming
 255 a constant cross-shore seabed slope sl and the horizontal distance between the
 256 shoreline position $y(t)$ and the tip of the groyne, where the water-depth $D_G(t)$ is taken
 257 into account (Fig. 9). Subsequently, $D_G(t)$ is given by Eq. (13):

$$258 \quad D_G(t) = sl(y_{GB} + L_G - y(t)) \quad (13)$$

259 where L_G is the groyne's length measured from the point it intersects the initial
 260 shoreline up to the groyne's seaward tip, y_{GB} is the distance from the shore-ward end
 261 of the groyne (namely, the point where the initial shoreline intersects the groyne) to
 262 the x -axis, and $y(t)$ is the shoreline position at time t , (Fig. 9). The physical meaning
 263 of Eq. (13) is that as the shoreline near the groyne changes in time, the depth $D_G(t)$ is
 264 expected to change as well.

265 Figure 9

266 The horizontal distance between the shoreline at the groyne and the calculated
 267 depth of active longshore transport is denoted by y_{LT} , (Fig. 9). $y_{LT}(t)$ describes the
 268 cross-shore zone of active longshore sediment transport. $y_{LT}(t)$ is expected to alter in
 269 time as the shoreline evolves, and consequently, the depth of active longshore
 270 transport, $D_{LT}(t)$, changes due to the time-varying hydrodynamic forcing (Eq. (12)).
 271 Thus, $y_{LT}(t)$ is given via Eq. (14):

$$272 \quad y_{LT}(t) = \frac{D_{LT}(t)}{sl} \quad (14)$$

273 Bypassing will occur under the following condition given from Eq. (11), namely
 274 $D_{LT}(t) > D_G(t)$. This condition ensures that the active water-depth D_{LT} is greater than
 275 the water-depth at the groyne so that sediment bypassing can occur.

276 Thus, the portion of longshore sediment flux ra that bypasses a groyne is given by Eq.
 277 (15):

$$278 \quad ra = 1 - \frac{L_G - (y(t) - y_{GB})}{y_{LT}(t)} \quad (15)$$

279 The physical meaning of Eq. (15) is that only the part of the cross-shore beach
 280 profile up to the depth of active longshore transport, which is not shadowed by the
 281 groyne, contributes to the bypassing process. Therefore, in the case where $y - y_{GB} = L_G$,
 282 in other words, the updrift side of the groyne is full, then, $ra = 1$, and the full amount
 283 of sediment flux passes from the updrift side of the groyne to the downdrift, while, if
 284 $y_{LT} \leq L_G - (y - y_{GB})$, namely, the whole zone of active longshore transport y_{LT} is
 285 shadowed by the groyne, then, $ra = 0$, and no bypassing takes place.

286 With the above assumptions, an internal impermeable groyne of finite length
 287 may be simulated according to the following boundary condition:

$$288 \quad \frac{\partial y}{\partial x} = \alpha_0 (1 - ra) \quad (16)$$

289 where $\frac{\partial y}{\partial x}$ is the local gradient of the shoreline curve; and α_0 is the angle of breaking
 290 wave crests in relation to the shore normal.

291 In addition to the possibility of bypassing, sediment material might pass
 292 through the body of a groyne such as when it is made of rocks. Hanson (1989)
 293 proposed a relation to describe the total amount of sediment movement from the
 294 updrift to the downdrift side of the groyne:

$$295 \quad F = p(1 - ra) + ra \quad (17)$$

296 where F is the portion of the longshore sediment flow which passes to the downdrift
 297 side of a groyne; while p is the portion of the longshore sediment transport which
 298 corresponds to the permeability of the groyne.

299 Under the combined effect of sediment bypassing and permeability the
 300 internal boundary condition at the groyne is as follows:

$$301 \quad \frac{\partial y}{\partial x} = a_0(1 - F) \quad (18)$$

302 It should be noted that the condition described by Eq. (16) embodies a
 303 modification of the physics described by the more familiar impermeable condition.
 304 The physical meaning of Eq. (16), (and Eq. 18), can be understood as follows. In the
 305 case of an impermeable, infinitely long groyne all sediment transport past the groyne
 306 is halted. This is equivalent to the beach plan shape being parallel to the incoming
 307 wave crests. This doesn't prevent accumulation of sediment on the updrift beach but
 308 fixes the angle of the beach at the groyne. In a computational model based on a
 309 staggered grid, the transport rates are calculated at half-points while groynes are
 310 placed at whole points. A by-passing formula akin to Eq. (16) can thus be
 311 implemented by using the transport rates near but not at the groyne, (Hanson 1989). In
 312 an analytical model the boundary condition is implemented at the location of the
 313 groyne and a by-passing criterion embedded within it at this point. To represent by-
 314 passing the condition of zero transport must be modified. Within the constraints of the
 315 1-line model this require the beach plan shape gradient to be modified so that it is not
 316 parallel to the wave crests at the groyne. This was recognised by Larson et al (1997)
 317 who proposed a formula to mimic by-passing based on the fullness of the groyne (i.e.
 318 the proportion of the groyne length to which the beach on the updrift side had
 319 reached), that also adjusted the beach angle at the groyne.

320 For small wave angles the sediment transport rate along the shoreline is given
 321 by the following formula:

$$322 \quad Q = Q_0(2a_0 - 2\frac{\partial y}{\partial x}) \quad (19)$$

323 where Q_0 is the amplitude of longshore sediment transport rate. The combination of
 324 Eqs. (18) and (19) yields Eq. 20 which describes the sediment flow due to bypassing
 325 of sediment material around the seaward tip of an impermeable groyne:

$$326 \quad Q = 2a_0Q_0 F \quad (20)$$

327 Following the principle of continuity of mass, the sediment flow on the updrift side of
 328 the groyne is the same as on the downdrift side, thus, according to Eq. 21:

$$329 \quad Q^{up} = Q^{down} \Rightarrow 2a_0Q_0F^{up} = 2a_0Q_0F^{down} \Rightarrow F^{up} = F^{down} \quad (21)$$

330 Therefore, from Eq. 18, it can be concluded that the boundary conditions on the
 331 updrift and the downdrift side of a groyne are the same whether bypassing takes place
 332 or not:

$$333 \left(\frac{\partial y}{\partial x}\right)_{up} = \left(\frac{\partial y}{\partial x}\right)_{down} \quad (22)$$

334 The semi-analytical solutions of Reeve (2006) and Zacharioudaki and Reeve (2008)
 335 may be used with the internal boundary conditions above and so may be used to
 336 include a sufficiently general form of boundary condition that encompasses beach
 337 evolution within a groyne field.

338 3. Evaluation of the analytical solution

339 To illustrate the type of situations in which the methodology described in
 340 Section 2 can be applied solutions for several cases are presented here. Calculations
 341 are performed for a period of one year. As test cases we consider two initial beach
 342 configurations: a straight, north-facing shorefront whose normal is $0^\circ N$; and a beach
 343 with the same orientation but with an initial Gaussian shape, given by the
 344 mathematical expression: $y(x, 0) = 50e^{-(x-5100)^2/500000}$. This initial condition
 345 corresponds to the following curve in the domain $0 m < x < 10200 m$ and is shown in
 346 Fig. 10.

347

348 Fig. 10. The convex initial beach condition.

349 Two forms of wave conditions have been used. The first is a sequence of
 350 weekly wave conditions over the one year period. These were created using the
 351 method described in Valsamidis and Reeve (2017) and the full set of conditions is
 352 provided in Appendix A. The summary statistics are provided in Table 1.

	Range of values	Mean value	Standard deviation
Wave height (Hs)	0m – 1.30m	0.52 m	0.22m
Wave Period (T)	1 sec – 12 sec	5.93 sec	2.02 sec
Wave direction (α)	-0.13 rad – 0.19 rad	0.04 rad	0.05 rad

353 Table 1: Statistical characteristics of the wave time-series.

354 The second wave condition is a constant one, consisting of the mean values of wave
 355 height, period and direction from the weekly sequence. The corresponding values are

356 shown in the second column of Table 1. The longshore sediment transport rate was
 357 calculated using the CERC longshore sediment transport formula (CERC, 1984),

$$358 \quad \varepsilon = \frac{K}{D_C + D_B} \left(\frac{C_{gb}}{8(s_g - 1)(1 - p_o)} \right) H_{sb}^2, \quad (23)$$

359 where K is a dimensionless calibration parameter depending on the special
 360 characteristics of the coastal system which is under investigation. Here, we set
 361 $K=0.39$ following the guidance in USACE (1984). D_c is the depth of closure taken
 362 equal to $6m$, D_B is the berm height which was set equal to $1m$; C_{gb} is the group
 363 velocity of the waves at breaking and s_g is the dimensionless magnitude of the specific
 364 gravity assigned the value 2.65 ; p_o is the porosity, set to 0.4 which is typical of sandy
 365 beaches; and H_{sb} is the significant wave height. Table 2 summarises the different
 366 cases for which results are shown.

Case No.	Initial condition	Wave condition	Groynes
1	Straight	Constant	Infinite, impermeable
2	Straight	Constant	Impermeable, by-passing
3	Straight	Constant	Permeable, by-passing
4	Gaussian	Constant	Infinite, impermeable
5	Gaussian	Constant	Impermeable, by-passing
6	Gaussian	Constant	Permeable, by-passing
7	Straight	Varying	Impermeable, by-passing
8	Gaussian	Varying	Impermeable, by-passing

367 Table 2: Summary of illustrative test cases.

368 In the first case, the initially straight beach is identical to the x -axis in a Cartesian
 369 system, and the y -axis measures the shoreline position relative to the x -axis, as shown
 370 in Fig. 11. This beach extends $10200 m$ in length and it includes a groyne field
 371 consisting of 3 groynes denoted Groyne 1, Groyne 2 and Groyne 3 located at $x =$
 372 $4650m$, $5100m$ and $5550m$ respectively. Each groyne extends $50 m$ in the offshore
 373 direction from the initial shoreline position, and also extends landward in the negative
 374 y -axis direction, to avoid undercutting. The seabed gradient is taken to be 1% . The
 375 external boundary conditions are free, allowing sediment material to enter and leave
 376 the domain.

377 Figure 11

378 The model was firstly evaluated for constant incident wave conditions that are the
 379 mean values of the wave time-series included in Table 1, namely, $H_s=0.52\text{ m}$; $T=5.93$
 380 sec ; and $\alpha=+0.04\text{ rad}$.

381 The first three cases listed in Table 2 correspond to this situation for,
 382 respectively: a) infinitely long impermeable groynes; b) sediment bypassing around
 383 the seaward tips of impermeable groynes; and c) sediment bypassing around the
 384 seaward tips of groynes which are considered to be 20% permeable.

385 The shoreline positions for these three cases, after 1 year, are shown in Figure 12.

386 Figure 12

387

388 The choice of a 1 year period is arbitrary but typical of the periods used for the
 389 type of simulation made using 1-line models. Figure 12 shows the qualitative
 390 behaviour that would be anticipated in the three different cases, with by-passing and
 391 permeability alleviating the ‘terminal groyne syndrome’ often encountered on the
 392 downdrift edge of groyne systems that interrupt the littoral drift. Figure 13 shows the
 393 time history of the transport rate at Groyne 3 over the one year period. This shows
 394 low rates initially, due to permeability. After a few weeks accumulation on the updrift
 395 side of the groyne is sufficient to activate some by-passing, which continues to
 396 increase slightly over the remainder of the period, demonstrating that an equilibrium
 397 state has not yet been reached.

398 Figure 13

399 The three groynes divide the domain into four sections, 1 to 4, from left to
 400 right. Thus Section 1 is $0\text{m} < x < 4650\text{m}$, Section 3 is $5100\text{m} < x < 5550\text{m}$ and so on.
 401 Table 3 summarises the net transport rates within the domain over the 1 year period,
 402 by quarter for Case 3. Results are quoted with units of $\text{m}^2/\text{yr}/\text{linear metre}$ and are
 403 calculated from the area change in each section, divided by the length of the section
 404 and the duration.

Period \ Region	Section 1	Section 2	Section 3	Section 4
Case 1				
1st Quarter	-1.72	0.00	0.00	1.72
2nd Quarter	-1.80	0.00	0.00	1.80

3rd Quarter	-1.80	0.00	0.00	1.80
4th Quarter	-1.80	0.00	0.00	1.80
Case 2				
1st Quarter	-0.75	0.00	0.24	0.72
2nd Quarter	-0.88	0.02	0.73	0.81
3rd Quarter	-0.88	0.06	0.99	0.78
4th Quarter	-0.88	0.10	1.17	0.76
Case 3				
1st Quarter	-0.61	0.00	0.03	0.60
2nd Quarter	-0.71	0.01	0.49	0.66
3rd Quarter	-0.70	0.03	0.66	0.64
4th Quarter	-0.70	0.05	0.79	0.62

405 Table 3. Net transport rates by quarter and section, ($\text{m}^2/\text{yr}/\text{m}$), for Cases 1 to 3.

406 For each quarter, summing the products of the quoted rate and the respective lengths
 407 of each section yields a value of effectively zero, (to rounding error), confirming the
 408 overall conservation of sediment. The rates for the first quarter are slightly below
 409 those for the remaining quarters due to inaccuracies in evaluating Eq. (2 & 4) for very
 410 small values of t .

411 The corresponding shoreline positions after 1 year for Cases 4 to 6 are shown
 412 in Fig. 14 and the net transport rates in Table 4.

413 Figure 14

Period \ Region	Section 1	Section 2	Section 3	Section 4
Case 4				
1st Quarter	-1.57	0.00	0.00	1.44
2nd Quarter	-1.84	0.00	0.00	1.76
3rd Quarter	-1.84	0.00	0.00	1.76
4th Quarter	-1.84	0.00	0.00	1.76
Case 5				
1st Quarter	-0.84	-0.22	0.70	0.66
2nd Quarter	-0.89	-0.31	0.20	0.83
3rd Quarter	-0.90	-0.29	0.26	0.82
4th Quarter	-0.90	-0.27	0.28	0.82
Case 6				
1st Quarter	-0.71	-1.16	1.24	0.57
2nd Quarter	-0.73	-0.40	0.24	0.67
3rd Quarter	-0.73	-0.18	0.03	0.67
4th Quarter	-0.73	-0.17	0.02	0.66

414 Table 4. Net transport rates by quarter and section, ($\text{m}^2/\text{yr}/\text{m}$), for Cases 4 to 6.

415 In this case the diffusion of the initial hump across the boundaries of the finite
 416 domain will result in the net loss of sediment from the domain. The semi-analytical
 417 solutions are valid on an infinite domain so the apparent sediment loss arises from
 418 performing the calculations on a finite portion of the infinite domain which does not
 419 fully contain the disturbance of the beach from a straight line. The initial condition
 420 introduces an asymmetry into the problem with outward spreading of the hump is
 421 combined with wave-driven transport from left to right in Figure 14. As a result the
 422 transport rates in Section 1 and 4 are not equal and opposite as for the initially straight
 423 beach, which results in rapid erosion in the lee of Groyne 1, even with permeable
 424 groynes and by-passing occurring.

425 Finally, the shoreline response after 1 year for Cases 7 and 8, for a randomly
 426 varying wave climate described in Table 1, are shown in Figure 15.

427 Figure 15

428

429 The instantaneous transport rates at Groyne 3 for Case 8 are plotted in Figure 16 and
 430 illustrate intermittent drift reversal throughout the year. Net transport rates for cases 7
 431 and 8 are presented in Table 5.

432 Figure 16

433

434

Period \ Region	Section 1	Section 2	Section 3	Section 4
Case 7				
1st Quarter	-1.83	0.00	1.38	1.70
2nd Quarter	-1.26	-0.93	2.92	1.03
3rd Quarter	-0.15	-0.87	0.74	0.19
4th Quarter	-0.26	-0.25	0.60	0.25
Case 8				
1st Quarter	-1.83	-0.62	0.87	1.68
2nd Quarter	-1.23	-1.78	2.11	1.10
3rd Quarter	-0.11	-1.54	-0.04	0.25
4th Quarter	-0.24	-0.81	-0.10	0.29

435 Table 5. Net transport rates by quarter and section, ($m^2/yr/m$), for Cases 7 and 8.

436

437

438

439 **4. Discussion**

440 Semi-analytical solutions for beach evolution within a groyne field have been
441 presented. The range of situations for which analytical solutions can be derived has
442 been extended to include an extended groyne field in which the initial shoreline shape
443 is not restricted to be straight, the groynes may be permeable and of finite length
444 which allows by-passing. The shoreline response to wave forcing, as predicted by the
445 new semi-analytical solution is in agreement with physical considerations sediment
446 transport and sediment conservation. For instance, in Fig.12 accretion is observed on
447 the updrift side of the groynes and erosion on the downdrift side. Moreover,
448 depending on the internal boundary condition, namely, absolute blockage of sediment
449 transport; impermeable groyne with sediment by-passing; or permeable groyne with
450 sediment by-passing, the amount of accretion observed on the updrift side of the
451 groynes decreases, respectively, and as a result, the amount of erosion on the
452 downdrift side of the groynes decreases proportionally. Also, in the case where the
453 groynes are permeable or by-passing the start of sequential filling of the groyne
454 compartments is evident, in accordance with the direction of the longshore transport.
455 This process is far from completed and the beach configuration shown in Fig. 12 is
456 not an equilibrium state, as evident from the sediment transport rates, (Fig. 13), which
457 show a continuing but gradual rise after one year.

458 The case where the beach shape is not a straight line introduced some
459 interesting features. It may be noticed that in Fig.14 the amount of accretion on the
460 updrift side of Groynes 3 and 2 with the Gaussian initial shoreline appears smaller
461 than the corresponding amount of accretion for the case of an initially straight
462 shoreline. Further, the magnitude of erosion on the downdrift side of Groyne 1 is
463 larger for Case 1 than Case 2. These observations may be explained by the diffusive
464 behaviour of the One-Line model Eq. (1) which tends to smooth salients formed along
465 the shoreline. Specifically, the peak of a salient retreats over time towards the baseline
466 while at locations on its flanks may experience accretion due to the sideways
467 spreading, (Larson et al. 1987). To amplify this point, Case 1 which is illustrated in
468 Fig.14 was repeated with the wave direction fixed so that $\alpha=0$, and the internal
469 boundary conditions set to impermeable groynes of theoretically infinite length. The
470 shoreline will evolve to align itself to the incoming wave crests. The beach in the

471 groyne compartments straightens while the beach outside this area spreads, with the
472 peak retreating fastest and the flanks accreting slightly, as shown in Fig.15.

473 Figure 15

474 All results show that there is greater accumulation of sediment material in the
475 first groyne compartment encountered by the predominant longshore drift, namely
476 between Groynes 2 and 3, than in the subsequent groyne compartment, defined by
477 Groynes 1 and 2. This arises from the greater sensitivity of the beach response to the
478 groyne that first intercepts the longshore transport. This phenomenon can be
479 understood physically from the greater mobilization and supply of sediment in an area
480 with an open boundary as opposed to a groyne compartment in which the supply of
481 sediment is more confined. Thus, when sediment material is allowed to pass from the
482 one compartment to another, (for instance Cases 2 and 3 in Fig.12), more sediment
483 material may be entering the updrift groyne compartment (the area between Groynes
484 2 and 3) than leaving. In contrast, there is an approximate balance in sediment
485 material entering and exiting the downdrift groyne compartment (between Groynes 1
486 and 2). This is apparent in Fig.12 (cases 2 and 3), where the shoreline position is
487 almost the same for all the 3 cases, indicating that there is virtually no net sediment
488 material accumulation or loss. One way to produce an accretion trend in the second
489 groyne compartment (the area between Groynes 1 and 2) would be to decrease the
490 permeability of Groyne 1 to prevent sediment material from exiting this groyne
491 compartment. Thus, Case 3 which is illustrated in Fig.12, was slightly altered
492 considering the permeability to be $p=0$ at Groyne 1. The resulting calculation
493 produced the complementary Case 3* which is plotted versus Case 3 in Fig.16.

494 Figure 16

495 Fig. 16 shows that if Groyne 1 is impermeable then accretion occurs on its updrift
496 side, however, the terminal groyne effect (Fig. 3) is exacerbated on the downdrift
497 side.

498 The concept of varying the permeability of groynes is being implemented in a
499 new generation of groynes which can be adjusted to the prevailing morphodynamic
500 conditions (e.g. MENA Report, 2014). An example is shown in Fig. 17. This type of
501 structure will have a permeability that varies with beach position, and therefore with
502 time.

503 Figure 17

504 Just such behaviour can be incorporated directly into the new semi-analytical
505 solution through the time varying internal boundary conditions. (In this regard it is
506 worth noting that the sediment movement through a permeable groyne is activated in
507 the modelling process only when $y(t)-y_{GB}(t)>0$.)

508 Finally, a comparison between the beach response to constant wave conditions
509 and varying wave conditions, (comparing Figs. 11 and 14 with Fig. 15), shows that
510 including for the occurrence of temporary drift-reversal ameliorates the beach
511 response.

512 **5. Conclusions**

513 One limitation of analytical solutions has been their applicability solely to
514 simple situations such as a single groyne or single groyne compartment. In this paper
515 we have proposed a means of accounting for sediment transmission through
516 permeable groynes and by-passing groynes of finite length under time varying wave
517 conditions. The underlying concept is based on the concept of the instantaneous active
518 depth of longshore transport introduced by Hanson (1989) for computational
519 modelling; modified to account explicitly for non-zero transport at the groyne by
520 adjusting the gradient of the beach planshape at the groyne according to the extent of
521 the active depth beyond the groyne tip. This has provided an analytical means of
522 calculating the beach plan shape evolution in a groyne field consisting of an arbitrary
523 number of groynes, which represents a considerable increase in the complexity of
524 beach configurations amenable to analytical treatment.

525 The internal boundary conditions have been combined with the solutions for
526 shoreline evolution near a groyne (Reeve, 2006) and shoreline evolution in a groyne
527 compartment (Zacharioudaki and Reeve, 2008). A range of solutions have been
528 presented to illustrate the type of situations that may be modelled. These are all based
529 on a one year period with a groyne field comprising three groynes in which the
530 groynes were impermeable and of infinite length; impermeable and of finite length,
531 permitting sediment bypassing; permeable and of finite length permitting bypassing.
532 Two initial beach conditions were also considered: a straight shoreline and a
533 Gaussian-shaped curve that mimicked a large nourishment or ness. Two forms of

534 wave condition were considered: constant, as commonly assumed in early analytical
535 solutions; and time-varying on a weekly basis.

536 The solutions capture the qualitative beach behaviour observed in practice.
537 Quantitative results have also been provided, expressed as instantaneous and net
538 transport rates. The different internal boundary conditions mimic the effect of
539 impermeable and permeable groynes, as well as by-passing. The description of these
540 processes is a simplified version of reality that is consistent with the 1-line concept.
541 One caveat of the method is that it can be difficult to evaluate for very small time
542 periods; in the cases studied here this equated to periods of a week or less. However,
543 as the 1-line concept is applied to problems simulating periods of months to years this
544 is not seen as a major impediment. The methodology proposed in this paper also
545 provides the means to develop new analytical solutions of more complicated
546 situations for testing computational models.

547

548 **Acknowledgements**

549 The support of the UK Engineering and Physical Sciences Research Council (EPSRC)
550 under the MORPHINE project (grant EP/N007379/1) is gratefully acknowledged.

551

552 **Appendix A. Wave time series used as input-data to the semi-analytical solution**

Wave Height (m)	Wave Period (sec)	Wave Direction (rad)
0.39	3.5	0.04
0.20	2.3	-0.09
0.55	3.4	0.01
0.98	5.1	0.17
0.42	4.8	0.19
0.12	2.2	-0.14
0.46	3.1	0.10
0.73	3.9	0.07
0.96	4.9	0.16
0.67	4.0	0.16
1.08	5.1	0.18
0.66	3.8	0.22
0.61	4.4	0.01
0.35	4.3	0.17

0.74	3.9	-0.09
0.37	3.4	-0.04
0.17	2.6	-0.03
0.76	4.0	0.24
0.57	4.3	0.13
0.73	3.8	0.28
0.29	2.7	0.18
0.59	3.8	0.14
0.82	4.6	0.17
0.57	3.6	0.08
0.66	3.6	0.13
0.83	4.2	0.18
0.86	4.7	0.07
1.08	5.4	0.03
0.96	4.8	0.16
1.11	5.6	0.17
0.88	4.6	0.04
1.00	5.4	-0.02
1.10	5.2	0.04
1.02	5.1	0.12
1.22	6.4	0.21
0.98	5.2	0.18
1.04	5.7	0.04
0.33	1.8	0.09
0.42	2.8	0.04
0.96	5.2	0.16
0.25	1.3	-0.02
0.22	2.3	0.05
0.93	4.8	0.13
0.92	5.1	0.18
1.04	6.0	0.12
0.57	4.6	0.11
0.58	4.1	-0.09
0.42	2.6	-0.03
0.79	4.4	0.16
0.93	5.1	0.12
0.42	2.7	0.06
0.76	4.5	0.09

553

554 **References**

555 Bakker, W.T., 1969. The dynamics of a coast with a groyne system. Proc 11th Coastal Engrg
556 Conf., ASCE, New York, N.Y. pp. 492–517.

557

- 558 Basco, D.R., Pope, J., 2004, Functioning and Design of Coastal Groins: The Interaction of
559 Groins and the Beach—Process and Planning: Journal of Coastal Research, v. WINTER
560 2004, p. 121-130.
561
- 562 Birkemeier, W.A., 1985. Field data on seaward limit of profile change, Journal of Waterway,
563 Port, Coastal and Ocean Engineering, ASCE, 111(3), p598-602.
564
- 565 CERC, 1984, Shore protection manual: Vicksburg, Coastal Engineering Research Center, U.
566 S., Corps of Engineers.
567
- 568 Coghlan, I., Carley, J., Cox, R., Davey, E., Blacka, M., Lofthouse, J., 2013, Concept Designs
569 for a groyne field on the far north SSW coast: 22nd NSW Coastal Conference: Port Macquarie,
570 New South Wales.
571
- 572 Clarke, J., Milburn, C., Stevens, A., Townsend, D., Dowsett, H., Thomas, R., 2017, Regional
573 Beach Management Plan 2017: Littlehampton to Brighton Marina: Canterbury, Environment
574 Agency.
- 575 Fleming, C.A., 1990. Guide on the use of groynes in coastal engineering, CIRIA Report 119,
576 London, UK.
- 577 Gravens, M.B., Kraus, N.C., Hanson, H., 1991, GENESIS: generalized model for simulating
578 shoreline change: Report 2, Workbook and System User's Manual, U. S. Army Corps of
579 Engineers.
- 580 Hallermeier, R.J., 1983. Sand transport limits in coastal structure design, Proc. Coastal
581 Struct., 1983, ASCE, p703-716. Hanson, H., Bocamazo, L., Larson, M., Kraus, N.C., 2008,
582 Long-term beach response to groin shortening, Westhampton Beach, Long Island: New York:
583 International Conference on Coastal Engineering: Hamburg, Germany, ASCE, p. 1927-1939.
- 584 Hanson, H., 1987, GENESIS-A generalized shoreline change numerical model for
585 engineering use: Lund, Lund Inst. of Tech./Univ. of Lund.
- 586 Hanson, H., 1989, Genesis: A Generalized Shoreline Change Numerical Model: Journal of
587 Coastal Research, v. 5, p. 1-27.
- 588 Hanson, H. & Kraus, N.C., 1989. Genesis: Generalized Model for Simulating Shoreline
589 Change, Tech. Report, CERC-89-19, USACE, Washington, DC, 247pp.

- 590 Horikawa, K., Harikai, S. & Kraus, N.C., 1979. A physical and numerical modelling of
591 waves, current and sediment transport near a breakwater, Annual Reprot of the Engineering
592 Research Institute, University of Tokyo, No. 38, pp41-48.
- 593 Kraus, N.C., Hanson, H., Blomgren, S.H., 1994, Modern functional design of groin systems:
594 Coastal Engineering Kobe, Japan.
- 595 Larson, M., Hanson, H., Kraus, N.C., 1987, Analytical solutions of the one-line model of
596 shoreline change: Technical Report CERC-87-15, USAE-WES, Coastal Engineering
597 Research Center, Vicksburg, Mississippi.
- 598 Larson, M., Hanson, H., Kraus, N.C., 1997, Analytical solutions of one-line model for
599 shoreline change near coastal structures: Journal of Waterway Port Coastal and Ocean
600 Engineering, v. 123, p. 180-191.
- 601 MENA Report, 2014, Cortez groins removal and replacement project: Tender documents:
602 T24356360, Albawaba (London) Ltd.
- 603 Pelnard-Considère, R., 1956, Essai de théorie de l'évolution des formes de rivage en plages de
604 sables et de gâlets: Societe Hydrotechnique de France, IV'ème Journees de L'Hydraulique
605 Question III, rapport 1, p. 74-1-10.
- 606 Perlin, M. & Dean, R.G., 1979. Prediction of beach planforms with littoral controls. Proc
607 Coastal Structures '79, ASCE, pp792-808.
- 608 Perlin, M., Dean, R.G., 1983. A Numerical Model to Simulate Sediment Transport in the
609 Vicinity of Structures, Report, MR-83-10, US Army Corps of Engineers. Reeve, D.E., 2006,
610 Explicit Expression for Beach Response to Non-Stationary Forcing near a Groyne: Journal of
611 Waterway, Port, Coastal, and Ocean Engineering, v. 132, p. 125-132.
- 612 Reeve, D.E., Valsamidis A., 2014, On the stability of a class of shoreline planform models,
613 Coastal Engineering, v. 91, p. 76-83.
- 614 Shibutani, Y., Kuroiwa, M., Matsubara, Y., Kim, M., Abualtaef, M., 2009. Development of
615 N-line numerical model considering the effects of beach nourishment. J. Coastal Res. SI 56,
616 554–558. Steetzel, H.J., De vroeg, H., Van Rijn, L.C., Stam, J.L., 1988, Morphological
617 modelling using a modied multi-layer approach: International Conference on Coastal
618 Engineering: Copenhagen, Denmark, pp 1927-1939, ASCE.
- 619 USACE, 2002, Coastal Engineering Manual (CEM): Washington, DC 20314-1000, U.S.
620 Army Corps of Engineers. Valsamidis, A., 2016, A Comparative Study of New Beach

- 621 Modelling Techniques: PhD Thesis, College of Engineering / Swansea University, Swansea,
622 147 p.
- 623 Valsamidis, A., Cai, Y., Reeve, D.E., 2013, Modelling beach-structure interaction using a
624 Heaviside technique: application and validation: Journal of Coastal Research p. 410 - 415.
- 625 Valsamidis, A. Reeve, D.E., 2017, Modelling shoreline evolution in the vicinity of a groyne
626 and a river: Continental Shelf Research, v. 132, p. 49-57. Walton, T.L., 1994. Shoreline
627 solution for tapered beach fill, J Waterway, Port, Coast., and Oc. Engrg, ASCE, 120(6), 651-655.
- 628 Walton Jr, T.L., Dean, R.G., 2011, Shoreline change at an infinite jetty for wave time series:
629 Continental Shelf Research, v. 31, p. 1474-1480.
- 630 Wind, H.G., 1990. Influence functions, Proc. 21st Intl. Conf. Coastal Engrg, ASCE, Costa-del-
631 Sol, Malaga, Spain, 3281-3294.
- 632 Zacharioudaki, A., Reeve, D.E., 2008, Semianalytical Solutions of Shoreline Response to
633 Time-Varying Wave Conditions: Journal of Waterway, Port, Coastal, and Ocean Engineering,
634 v. 134, p. 265-274.

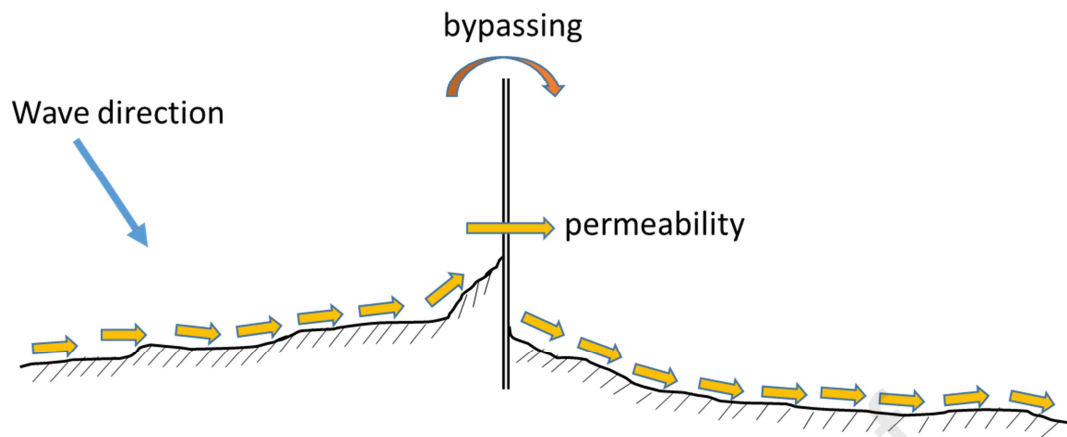


Fig. 1. For a specific direction of the littoral drift (shown by the orange arrows along the beach), accretion is caused on the updrift side of the groyne (denoted by the vertical double line) and erosion downdrift-wards. Sediment material is illustrated to pass through the body of the groyne, and to bypass its tip.

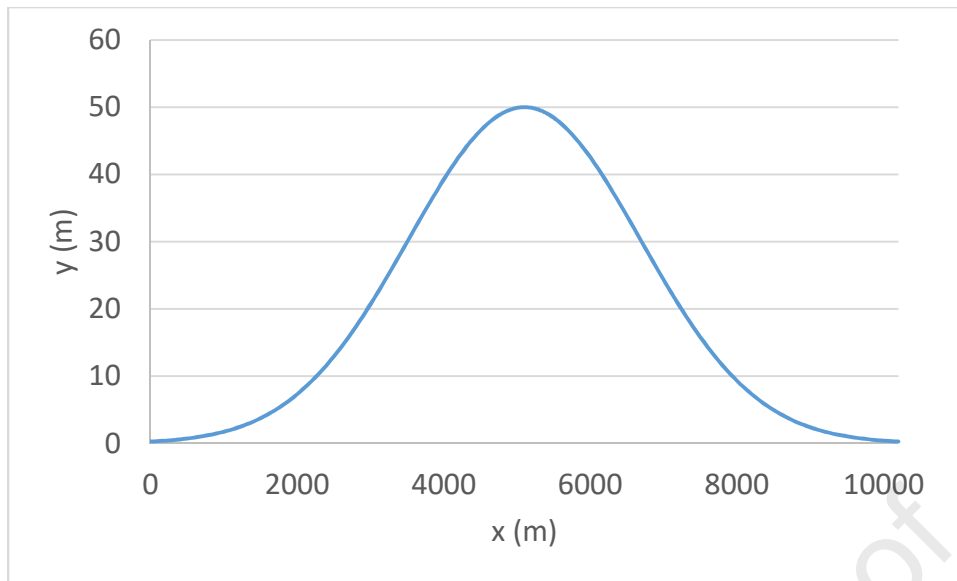


Fig. 10. A Gaussian curve was chosen as an initial condition in the modelling process, alternatively to an initially straight shoreline position.

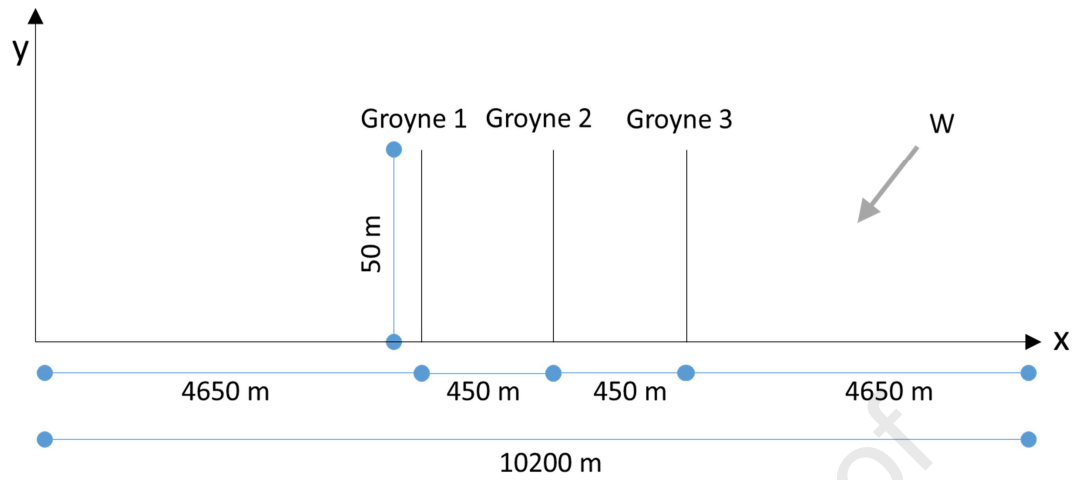


Fig. 11. The modelled area is characterized by free boundary conditions at $x=0$ m and $x=10200$ m, and 3 groynes in the middle, obstructing sediment transport along the shore.

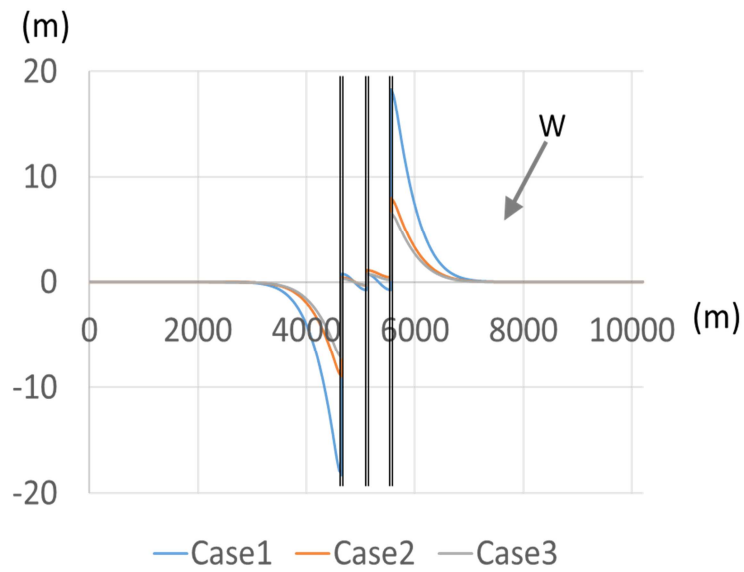


Fig. 12. The double vertical lines symbolize the 3 groynes. Three different scenarios are shown: impermeable groynes with no by-passing (blue); impermeable groynes with by-passing (orange); and permeable groynes with by-passing (grey).

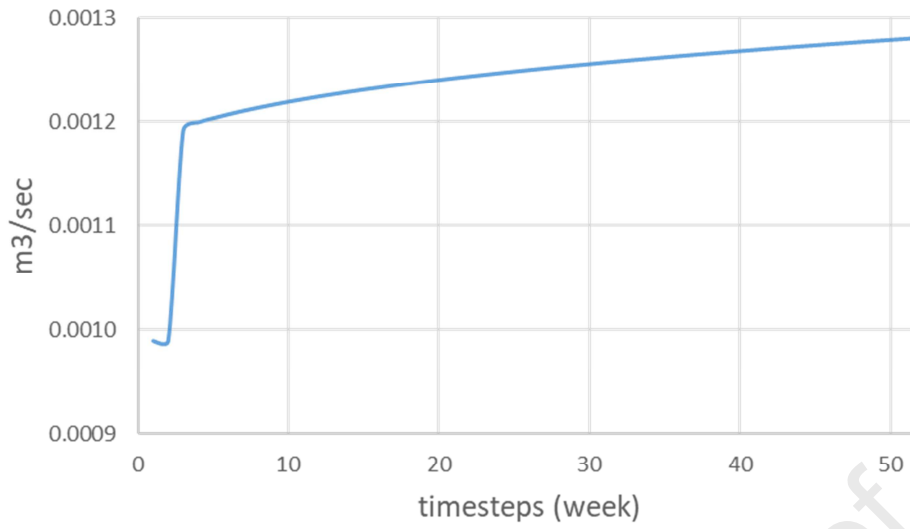


Fig. 13. Time history of the sediment transport rate at Groyne 3 in Case 3.

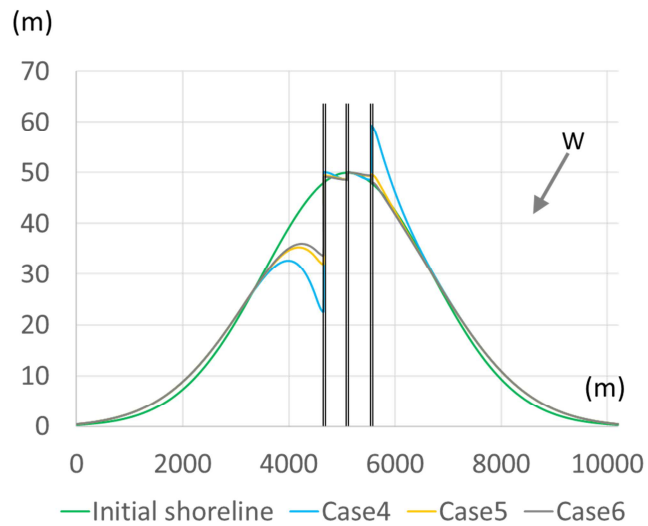


Fig. 14. Shoreline position at the end of 1 year for Cases 4 to 6. The Gaussian-shaped initial shoreline position is depicted with a green line. The double vertical lines symbolize the 3 groynes. Three different cases are shown: impermeable groynes with no by-passing (blue); impermeable groynes with by-passing (orange); and permeable groynes with by-passing (grey).

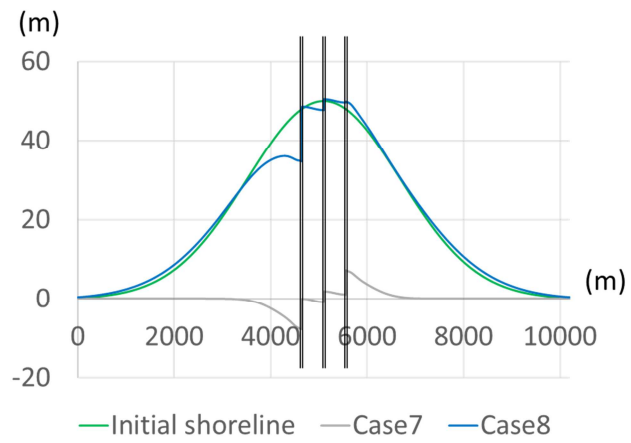


Fig. 15. Shoreline positions after 1 year for Cases 7 and 8. The wave conditions are described in Table 1, and the internal boundary conditions correspond to permeable groynes allowing bypassing.

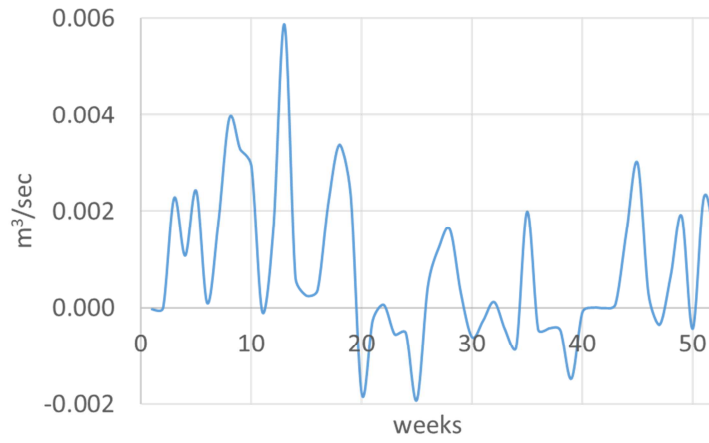


Figure 16. The instantaneous transport rates at Groyne 3 for Case 8.

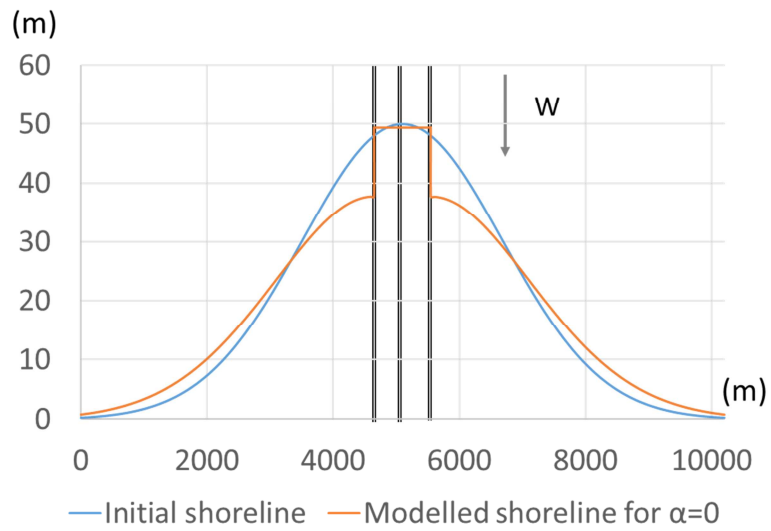


Fig. 17. Shoreline evolution after 1 year of an initially Gaussian shaped shoreline, for wave direction $\alpha=0$ and impermeable groynes, (denoted with double vertical lines).

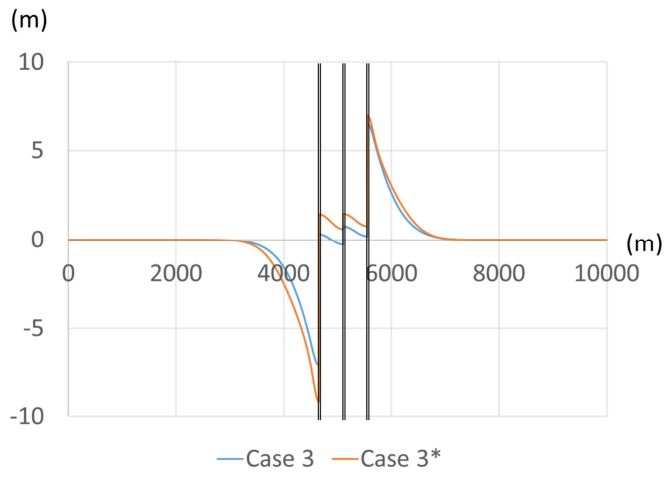


Fig. 18. Case 3* is the same as Case 3 except for the fact that Groyne 1 is impermeable.



Fig. 19. The innovative groyne design concept that allows for adjustment of groyne permeability by adding/removing pre-cast concrete blocks (photo: Cortez beach, Florida).

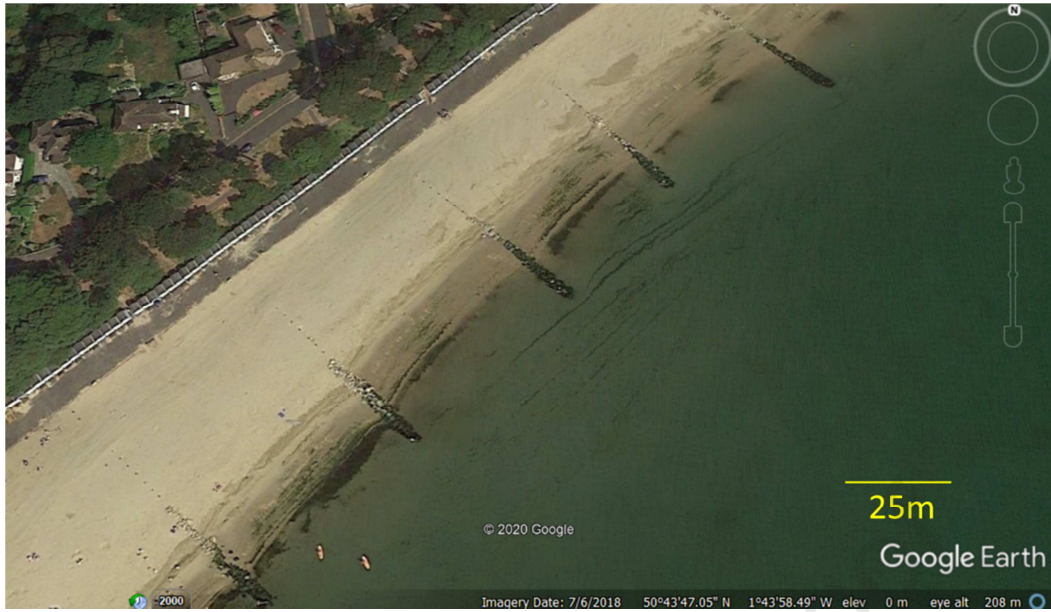


Fig. 2. Groyne field in Mundeford, England (extracted from Google Earth)



Fig. 3. (a) The terminal groyne syndrome occurring in Southwick beach in West Sussex where the net littoral drift is from left to right. (b) The same phenomenon is observed in Westhampton beach in New York where the net littoral drift is from right to left (photos extracted from Google Earth).

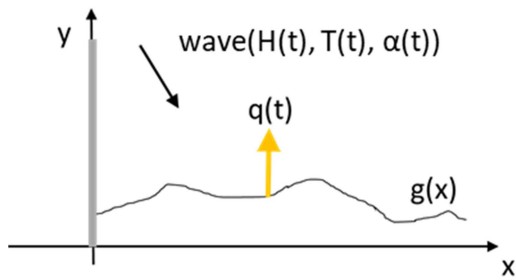


Fig. 4: The grey, vertical bar on the y axis symbolizes a groyne; $g(x)$ refers to the initial shoreline position, wave time-series of wave height $H(t)$, wave period $T(t)$ and wave direction $\alpha(t)$ can be incorporated as input-data to the semi-analytical model, as well as a time-varying sediment flow $q(t)$ from a source (in case $q > 0$) or sink (in case $q < 0$) of sediment discharge.

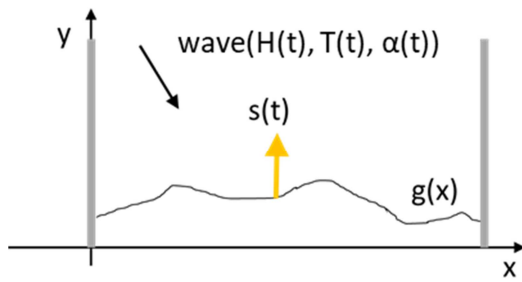


Fig. 5: The two vertical, grey bars denote the two groyne compartments that confine a beach section having initial shoreline position $g(x)$. Apart from a time-varying wave forcing, the groyne compartment might be imposed to a source or sink of sediment material with sediment flow $s(t)$.

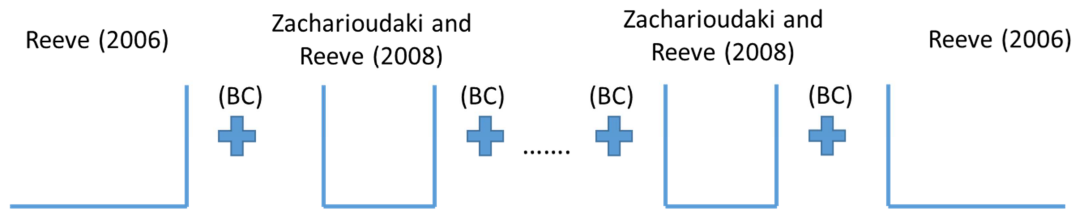


Fig. 6. With the proper internal boundary, the semi-analytical models can be combined to describe a groyne field.

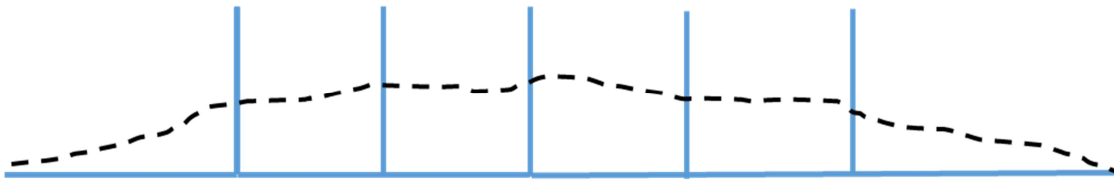


Fig. 7. A groyne field comprising of 5 groynes, and open external boundary conditions. The black intermittent line corresponds to the initial shoreline position.

Journal Pre-proof

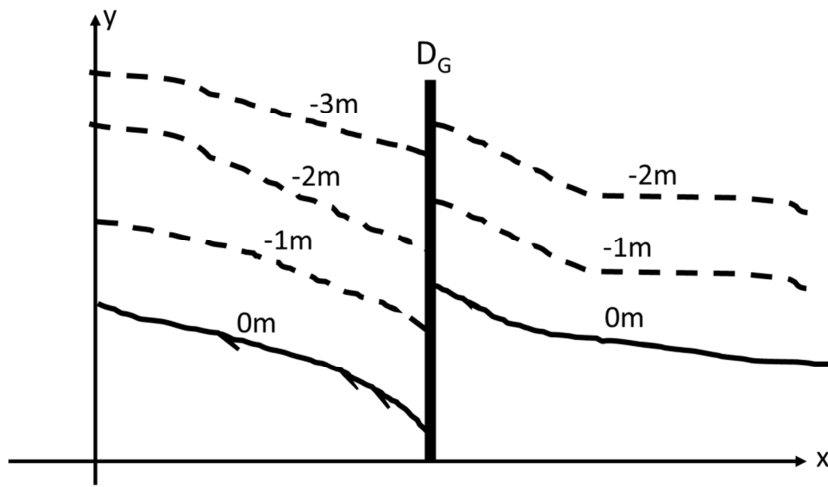


Fig. 8. The morphodynamic evolution on the updrift and downdrift side of a groyne alter the water depth D_G at the tip of the groyne. The solid line corresponds to the shoreline and the intermittent lines to the bathymetric contours.

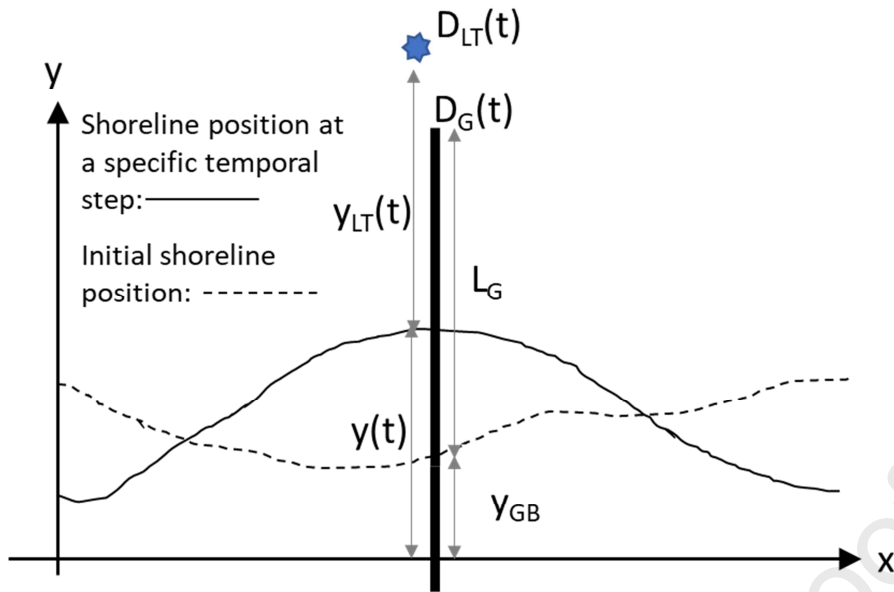


Fig. 9. Schematic illustration of the internal boundary condition introduced in this study

Highlights:

- New analytical solutions are derived for extended groyne fields
- Solutions are constructed from existing solutions and novel internal boundary conditions
- Solutions include littoral drift, groyne by-passing and groyne permeability
- Solutions are extended to allow time varying waves and arbitrary initial beach shape
- Practical example applications of the new solution are provided

Journal Pre-proof

Declaration of interests

The authors declare that they have no known competing financial interests or personal relationships that could have appeared to influence the work reported in this paper.

The authors declare the following financial interests/personal relationships which may be considered as potential competing interests:

Journal Pre-proof